REFERENCES AND NOTES

1. J. C. Wilson, J. H. Hyun, E. D. Blackshear, *J. Geophys. Res.* **88**, 6781 (1983).
2. The FCAS was calibrated with aerosol having a refractive index very near that of the measured particles. The inlet system (*10*) samples particles from the free stream and transports them to the FCAS for measurement. Sampling artifacts such as anisokinetic sampling and evaporation of water from particles due to heating in sampling and transport are accounted for in the data analysis. It is assumed that the aerosol is a liquid solution of sulfuric acid and water in equilibrium with the ambient water vapor. The reported size distributions reflect ambient conditions and include the water lost as a result of evaporation.
3. D. Baumgardner, J. E. Dye, B. W. Gandrud, R. G. Knollenberg, *J. Geophys. Res.* **97**, 8035 (1992). The FSSP-300 senses particles with minimal disturbance to the free stream and, hence, minimal alteration. Both the FSSP-300 and FCAS measure particles in the diameter range from 0.4 to ~3 μm. Simultaneous FSSP-300 and FCAS measurements of aerosol concentrations in this diameter range typically differ by from a few percent to a factor of 2. This difference is small compared to the dynamic range of aerosol concentrations observed. Measurements made in the volcanic cloud when most particles were of such a size as to be detected by all three instruments were similar.
4. M. P. McCormick and R. E. Veiga, *Geophys. Res. Lett.* **19**, 155 (1992); T. Deshler, D. J. Hofmann, B. J. Johnson, W. R. Rozier, *ibid.*, p. 199; M. J. Post, C. J. Grund, A. O. Langford, M. H. Proffitt, *ibid.*, p. 195.
5. G. J. S. Bluth, S. D. Doiron, C. C. Schnetzler, A. J. Krueger, L. S. Walter, *ibid.*, p. 151; L. A. Capone *et al.*, *ibid.* **10**, 1053 (1983); J. C. Wilson, E. D. Blackshear, J. H. Hyun, *ibid.*, p. 1029; S. A. McKeen, S. C. Liu, C. S. Kiang, *J. Geophys. Res.* **89**, 4873 (1984); D. J. Hofmann and J. M. Rosen, *Science* **222**, 325 (1983); R. P. Turco, R. C. Whitten, O. B. Toon, *Rev. Geophys. Space Phys.* **20**, 233 (1982).
6. K. T. Whitby, *Atmos. Environ.* **12**, 135 (1978). We determined N_a by fitting the surface distributions in Fig. 2 with lognormal functions and converting from the surface parameters to number concentration. We then determined N_n by subtracting N_a from the ER-2 CNC concentration.
7. P. J. Sheridan, R. C. Schnell, D. J. Hofmann, T. Deshler, *Geophys. Res. Lett.* **19**, 203 (1992).
8. V. R. Oberbeck *et al.*, *ibid.* **10**, 1021 (1983).
9. D. J. Hofmann, *Science* **248**, 996 (1990).
10. J. C. Wilson *et al.*, *J. Geophys. Res.* **97**, 7997 (1992).
11. J. L. Gras and J. E. Laby, *ibid.* **86**, 9767 (1981).
12. D. J. Hofmann, J. M. Rosen, J. W. Harder, *ibid.* **93**, 665 (1988); J. C. Wilson *et al.*, *ibid.* **94**, 16437 (1989).
13. M. Mozurkewich and J. G. Calvert, *ibid.* **93**, 15889 (1988); J. M. Van Doren *et al.*, *J. Phys. Chem.* **95**, 1684 (1991); D. R. Hanson and A. R. Ravishankara, *J. Geophys. Res.* **96**, 17307 (1991).
14. J. M. Rodriguez, M. K. W. Ko, N. D. Sze, *Nature* **352**, 134 (1991); D. J. Hofmann and S. Solomon, *J. Geophys. Res.* **94**, 5029 (1989); G. Brasseur and C. Granier, *Science* **257**, 1239 (1992).
15. S. R. Kawa *et al.*, *J. Geophys. Res.* **97**, 7905 (1992).
16. W. H. Brune, D. W. Toohey, S. A. Lloyd, J. G. Anderson, *Geophys. Res. Lett.* **17**, 513 (1990).
17. Potential temperature, Θ, is used as a vertical coordinate in Fig. 3. $\Theta = T(1000/P)^{0.286}$, where P is pressure in millibars and T is temperature in kelvin. In the absence of heat transfer, air parcels move along surfaces of constant Θ.
18. The research done at the University of Denver was supported by NASA Upper Atmosphere Research Program grant NAG 2-458. The suggestions of reviewers and editors are gratefully acknowledged.

1 March 1993; accepted 17 June 1993

Stratospheric Meteorological Conditions in the Arctic Polar Vortex, 1991 to 1992

P. Newman, L. R. Lait, M. Schoeberl, E. R. Nash, K. Kelly,
D. W. Fahey, R. Nagatani, D. Toohey, L. Avallone, J. Anderson

Stratospheric meteorological conditions during the Airborne Arctic Stratospheric Expedition II (AASE II) presented excellent observational opportunities from Bangor, Maine, because the polar vortex was located over southeastern Canada for significant periods during the 1991–1992 winter. Temperature analyses showed that nitric acid trihydrates (NAT temperatures below 195 k) should have formed over small regions in early December. The temperatures in the polar vortex warmed beyond NAT temperatures by late January (earlier than normal). Perturbed chemistry was found to be associated with these cold temperatures.

The mechanism responsible for causing large perturbations in Arctic stratospheric chemistry has been established as heterogeneous processes on polar stratospheric clouds (PSCs) (*1*). It has been hypothesized that PSCs consist of various nitric acid hydrates, sulfuric acid aerosols, and water ice particles. These clouds tend to form at temperatures below 195 K (*2*), close to the temperature required for the condensation of NATs (*3*). Water ice particles form at temperatures near 188 K and are large enough to fall out of the stratosphere on short time scales. The settling of these ice particles reduces both water and nitrogen concentrations in the stratosphere (dehydration and denitrification, respectively), further perturbing the stratospheric photochemical balance. In this report, we characterize the thermal structure of the Arctic lower stratosphere during the Northern Hemisphere winter of 1991–1992 (AASE II) and contrast this with the corresponding data for the winter of 1988–1989 (AASE I). We will relate these cold temperatures to PSCs and discuss the impact of PSCs on the polar vortex chemistry during the winter period.

In early December 1991, the polar lower-stratospheric temperatures at the 460 K potential temperature (Θ) surface (*4*) were cold (<205 K), and by late December they had cooled by an additional 10 K (*5*). In early January 1992, the cold temperatures straddled the polar night boundary and were located near the vortex edge (*6*), with a minor warming that raised temperatures above 195 K in late January (Fig. 1). During 1989, the cold temperatures were located mainly in the polar night, well inside of the polar vortex boundary, with a major warming in February 1989 (*7, 8*).

We examined the relation between the 1991–1992 cold temperatures and the perturbed chemistry in the stratosphere by using back trajectories to estimate the coldest temperature experienced by air parcels 10 days before sampling by the National Aeronautics and Space Administration (NASA) ER-2 aircraft (*9*). We then used measured H_2O and derived HNO_3 data (*10*) to estimate the NAT phase transition temperature. High concentrations of chlorine monoxide (ClO) (in excess of 200 parts per trillion) marked air parcels that experienced heterogeneous chemistry on PSCs. The National Meteorological Center (NMC) temperatures observed on the back trajectories (Fig. 2) reveal that (i) at temperatures below the NAT phase transition concentrations of ClO were almost always high, (ii) at temperatures slightly above the phase transition there was some perturbed chemistry (but generally not to the same degree as at those points well below the phase transition), and (iii) at temperatures 6 K higher than the phase transition concentrations of ClO were low. Hence, NMC temperatures, combined with the estimates of NAT phase transitions, provide a conservative technique for inferring the presence of a PSC.

Because these cold temperatures in the NMC fields are linked to the perturbed chemistry observed by the ER-2 [most probably PSCs or the accelerated hydrolysis of chlorine nitrate ($ClONO_2$) at temperatures below 200 K], the ER-2 observations (*10, 11*) can be used to analyze the impact of cold temperatures on the polar

P. Newman, L. R. Lait, M. Schoeberl, National Aeronautics and Space Administration Goddard Space Flight Center, Code 916, Greenbelt, MD 20771.
E. R. Nash, Applied Research Corporation, Landover, MD 20785.
K. Kelly and D. W. Fahey, National Oceanic and Atmospheric Administration Aeronomy Laboratory, 325 Broadway, Boulder, CO 80303.
R. Nagatani, National Meteorological Center Climate Analysis Center, World Weather Building, Washington, DC 20233.
D. Toohey and L. Avallone, Department of Geosciences, Physical Sciences Annex 206, University of California, Irvine, CA 92717.
J. Anderson, Harvard University Atmospheric Research Project, Engineering Science Laboratory, 40 Oxford Street, Cambridge, MA 02138.

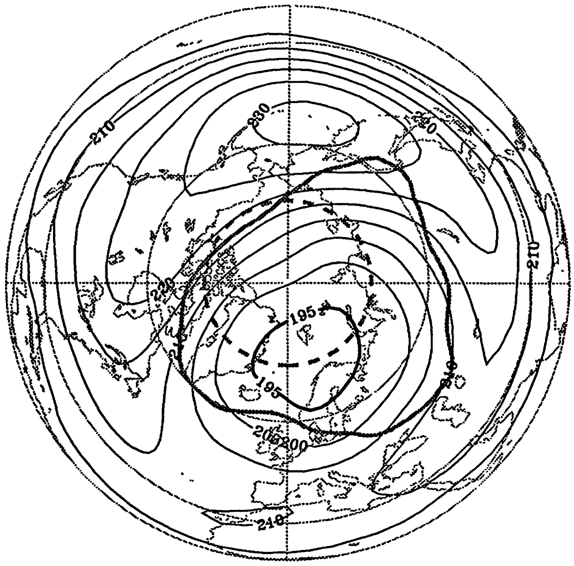

Fig. 1. NMC temperature average for 1 to 15 January 1989 on a 460 K isentropic surface. The 195 K contour (bold) indicates the region of PSC formation. The thick shaded line shows the vortex boundary and the dashed line shows the polar night boundary on 15 January.

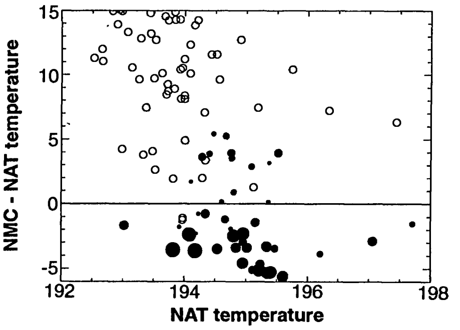

Fig. 2. Minimum NMC back trajectory temperature differenced with the calculated NAT saturation temperature. The difference is plotted versus the calculated NAT saturation temperature. The saturation temperature is calculated from the in situ ER-2 observations of H_2O and derived HNO_3 (*10*). Filled (open) circles indicate ClO values above (below) 200 ppt. Dot size is proportional to the ClO concentration.

vortex. We used the data to compute the range and average NAT phase temperatures on the 460 K surface (194.5 ± 2 K). When NMC temperatures fell below this phase transition and formed PSCs, we used the NMC and trajectory data to calculate the PSC area and the rate of processing by PSCs.

Polar temperatures grazed the NAT saturation line on 3 December 1991 and dropped significantly below the NAT line in late December (Fig. 3). During late January 1992, temperatures warmed significantly. Balloon observations show that temperatures were below the NAT line as late as 9 February and were cold enough to allow ice particle formation on 17 and 18 January 1992. However, NMC temperatures never fell below the frost point.

We used the 194.5 K (lower estimate: 193.5 K; upper estimate: 196 K) NAT phase transition temperature estimated from the ER-2 data on the 460 K Θ surface to calculate that NATs first appeared on 19 December 1991 (lower: 26 December; upper: 5 December) and the last day on which NATs were detected was 27 January 1992 (lower: 27 January; upper: 11 February). This gave a total of 40 days (lower: 33 days; upper: 69 days).

We used the trajectory model to analyze differences between the winters of 1988–1989 and 1991–1992 (*12*). The technique involves dividing the polar vortex region (defined by Ertel's potential vorticity values in excess of 2.5×10^{-5} K m^2 kg^{-1} s^{-1} on the 460 K surface) into equal areas on an equal-spacing grid. A parcel was placed at the center of each of these equal areas and run forward over the period during which PSCs could have formed. Both the 1988–1989 trajectories and the 1991–1992 trajectories were initialized on 10 December and were run forward to 18 February (70 days) (*13*).

The fraction of the vortex on the 460 K surface covered by PSCs was over 30% in 1991–1992 and up to 40% in 1988–1989 (Fig. 4). The error bars on the PSC vortex coverage range are rather large, extending from 14 to 37% in early January when the vortex coverage was 27%.

The fraction of air inside the vortex that passed through the PSC air at least once (the air was processed by PSCs) was over 90% by late January in both 1988–1989 and 1991–1992 (85% for the lower 193.5 K NAT temperature) (Fig. 5). In both cases, approximately 5% of the parcels escaped the vortex into mid-latitudes, where temperatures were too warm to permit the formation of PSCs. These processing rates are consistent with previous calculations performed with a three-dimensional transport code (*14*) and are independent of the chemical recovery time for recovery times greater than 2 weeks.

In early December 1991, the processing of the vortex was slow because the area covered by PSCs was small. However, the area of the vortex that had been processed increased rapidly in late December because PSCs covered 15% of the vortex and the PSC coverage was toward the vortex edge. When a PSC is located at the vortex edge (near the jet core), strong winds can move substantial amounts of air mass through the relatively stationary PSC formation region, thereby processing air. In 1988–1989 the processing was slower, because the PSC coverage was small early in the period, and the PSCs were located at the vortex center, where air tended to circulate within the cold region rather than moving through the region. The degree of processing by ice particles was low in both 1991–1992 and 1988–1989. In an average winter, cold temperatures persist from early December to mid-February; therefore, it seems probable that even relatively warm Northern Hemisphere winters will lead to virtually complete processing of the polar vortex. Calculations on other potential temperature surfaces (440 to 520 K) were similar. Above 520 K and below 440 K, temperatures were generally too warm to permit PSCs to form, so the effect of PSCs on the vortex at these altitudes was minimal.

We used the ensemble of 1991–1992 trajectories to estimate that 26% of the air in the vortex was below PSC temperatures for 3 days, while no air in the vortex spent more than 10 days as a PSC. On average, a parcel of air spent 2.8 ± 2.0 days at temperatures below PSC temperatures. In contrast, during 1988–1989 an average parcel of air spent 8.1 ± 5.0 days. Much of the 1988–1989 vortex air spent substantial time as PSCs, because air in the center of the vortex tended to cycle around inside the cold region rather than pass through the cold region, as was characteristic in 1991–1992. We also calculated that an average parcel of air in the 1991–1992 (1988–1989) vortex encountered 2.6 ± 1.2 (5.0 ± 2.2) PSCs over the course of the winter.

Because a 10-μm particle can fall 1 km in 3 days, ice particles should settle out of the stratosphere on short time scales, leading to denitrification and dehydration. Because temperatures were too warm for ice particles in 1991–1992, sedimentation by ice particles in the Northern Hemisphere should be relatively small in comparison to the Southern Hemisphere. In contrast, in 1988–1989 the vortex was partially denitrified. However, this ice particle sedimentation is highly conditional, because (i) the ice particle area is not well represented, (ii) particle size distributions are not sampled (sedimentation rates are a strong function of particle size), and (iii) subsynoptic cold temperatures are not resolved in the observational network.

Increased water or HNO_3 concentrations

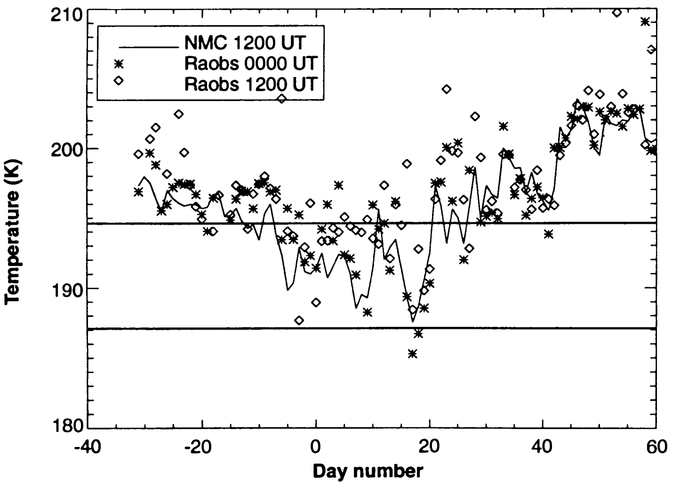

Fig. 3. Minimum temperature in the region 60° to 90°N. The solid line represents the NMC minimum temperature, and the stars and diamonds are from 0000 and 1200 UT raobs (radiosonde observations), respectively. The two horizontal solid lines represent the estimated NAT temperature (upper) and the frost point (lower).

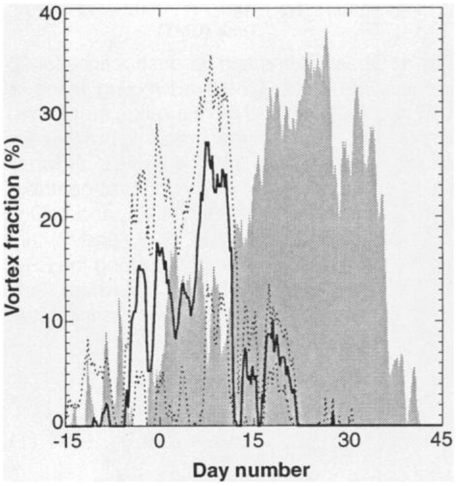

Fig. 4. The solid line (shaded region) shows the fractional PSC coverage on the 460 K surface of the polar vortex during 1991–1992 (1988–1989). The two dotted lines show the fractional coverage for extreme estimates of PSC saturation temperatures in 1991–1992.

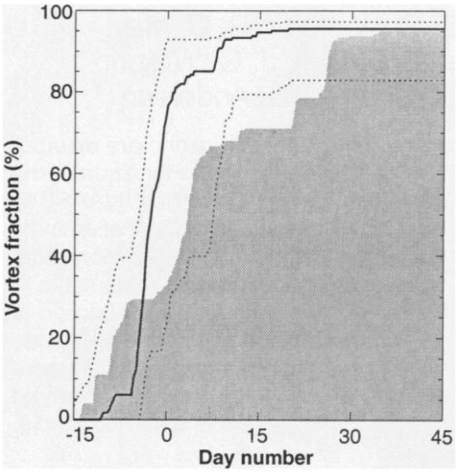

Fig. 5. The solid line (shaded region) shows the fractional PSC processing on the 460 K surface of the polar vortex during 1991–1992 (1988–1989). The two dotted lines show the fractional processing for extreme estimates of PSC saturation temperatures in 1991–1992.

will cause the PSC formation temperatures to increase. Water and HNO_3 increase because of increases in two source gases, CH_4 and N_2O (CH_4 is currently increasing at 0.8% per year, and N_2O at 0.2% per year) (*15*). We used the CH_4 trend to calculate an H_2O increase of 0.007 part per million by volume per year (*16*), while the HNO_3 increase is estimated as 0.009 ppb/year (*17*). These trends of H_2O and HNO_3 result in a yearly increase in the NAT phase transition temperature of 0.01 K. Hence, changes in the NAT phase transition and the consequent changes in PSC processing are small.

It is expected that direct injections of H_2O and NO_y (*18*) by future fleets of supersonic transports will lead to an increase of ~1.5 K in the NAT phase transition temperature (*19*) and a ~1.3 K increase in the frost point. These changes would dramatically alter the vortex. For example, imposing these increased HNO_3 and H_2O concentrations on the 1991–1992 winter would (i) extend the last day of NAT from 27 January to 9 February, (ii) increase by 10% the vortex coverage by NATs in midwinter, (iii) decrease vortex processing time scales by days, (iv) almost double the time spent by a piece of the vortex as a PSC, from 2.9 to 5.5 days, and (v) lead to the formation of a large region of ice particles on 18 January where none would have existed under current conditions, which would increase the denitrification of the vortex.

REFERENCES AND NOTES

1. J. Anderson, W. Brune, S. Lloyd, D. Toohey, *J. Geophys. Res.* **94**, 11480 (1989). See the Airborne Antarctic Ozone Experiment [*J. Geophys. Res.* **94**, 11179 (1989)] and AASE I [*Geophys. Res. Lett.* **17**, 313 (1990)] special issues. For an introductory article on PSCs, see P. Hamill and O. Toon [*Phys. Today* **44**, 34 (December 1991)].
2. M. P. McCormick *et al.*, *Geophys. Res. Lett.* **17**, 381 (1990); M. P. McCormick, H. M. Steele, P. Hamill, W. P. Chu, T. J. Swissler, *J. Atmos. Sci.* **39**, 1387 (1982).
3. D. Hanson and K. Mauersberger, *Geophys. Res. Lett.* **15**, 855 (1988).
4. Potential temperature (Θ) is the temperature an air parcel would have if adiabatically brought to a pressure of 1000 hPa. Under adiabatic conditions, parcels conserve potential temperature, eliminating vertical motion effects. The 460 K surface has an approximate altitude of 20 km and a pressure of 50 hPa (approximately the normal cruise altitude of the NASA ER-2).
5. The National Meteorological Center (NMC) Climate Analysis Center stratospheric data follows a long-term, consistent analysis scheme [G. P. Cressman, *Mon. Weather Rev.* **87**, 367 (1959)]. The scheme uses both satellite retrievals and balloon data [R. M. Nagatani, *Natl. Oceanic Atmos. Admin. (NOAA) Tech. Rep. NWS 40* (1988); W. J. Randel, *Natl. Cent. Atmos. Res. (NCAR) Tech. Note NCAR/TN-295+STR* (1987)]. See K. Trenberth and J. Olson [*Natl. Cent. Atmos. Res. (NCAR) Tech. Note NCAR/TN-299+STR* (1988)] for an evaluation of the tropospheric data. Winds and vorticities are calculated by means of a balanced wind scheme (*7*).
6. The polar vortex edge is calculated from the maximum gradient of Ertel's potential vorticity (Epv) on an isentropic surface.
7. P. A. Newman *et al.*, *Geophys. Res. Lett.* **17**, 329 (1989).
8. T. Fairlie *et al.*, *Q. J. R. Meteorol. Soc.* **116**, 767 (1990); B. Naujokat *et al.*, *Beil. Wetterkarte* **25**, 1 (1989).
9. C. Webster *et al.*, *Science* **261**, 1130 (1993); D. Toohey *et al.*, *ibid.*, p. 1134.
10. Scaled NO_y is used to derive HNO_3. The scaling factor (75%) is derived from the NASA Goddard Space Flight Center two-dimensional model using heterogeneous chemistry (D. Considine, personal communication) and is consistent with the fractional concentrations of HNO_3 calculated by S. R. Kawa *et al.* [*J. Geophys. Res.* **97**, 7925 (1992)] utilizing ER-2 data from the AASE I mission.
11. K. Kelly *et al.*, *Geophys. Res. Lett.* **17**, 465 (1989); S. Kawa *et al.*, *ibid.*, p. 485.
12. Isentropic trajectories, derived from NMC balanced winds, are checked against the conservation of Epv (*5*). Validation includes the simulation of volcanic clouds [M. Schoeberl *et al.*, *J. Geophys. Res.* **98**, 2949 (1993); see same for trajectory details]. Trajectories appear to be accurate up to a week, depending on flow conditions and analysis accuracy. At polar latitudes during winter, large zonal winds rapidly cause degradation of zonal accuracy as a result of wind errors. Integrations longer than 2 weeks are not accurate for determining zonal position. Latitudinal positions are more accurate, because zonal average meridional velocities are much smaller than zonal velocities. Thus, meridional position errors are small because of small absolute wind error. Latitudinal position can be accurately predicted but longitudinal position will be uncertain for 7- to 10-day integrations.
13. A 70-day forward trajectory is inconsistent with the 7- to 14-day validity of a "single" isentropic trajectory (*12*). However, it is not the "single" trajectory properties of the 70-day run that are of interest but the bulk properties of the entire ensemble. This technique has been used to calculate stratospheric mixing rates [H. Kida, *J. Meteorol. Soc. Jpn.* **61**, 510 (1983); L. Lyjak, *Transport Processes in the Middle Atmosphere* (Reidel, Dordrecht, the Netherlands, 1987), p. 343; M. R. Schoeberl, L. R. Lait, P. A. Newman, J. E. Rosenfield, *J. Geophys. Res.* **97**, 7859 (1993)]. The technique is directly validated by comparison to diagnostics from the meteorological fields: Epv conservation, cold temperature area, Epv advection, and thermal advection. In addition to these forward trajectories, back trajectories were run from 18 February to 10 December and show consistency with statistics derived from the forward trajectories.
14. J. Kaye *et al.*, *Geophys. Res. Lett.* **18**, 29 (1991).

15. "Scientific assessment of ozone depletion: 1991" [*Global Ozone Research and Monitoring Project Rep. 25* (World Meteorological Organization, Geneva, Switzerland, 1992)].
16. The H_2O trend is estimated by calculating the difference between the average H_2O with the H_2O residual estimated in K. Kelly *et al.* [*Geophys. Res. Lett.* **17**, 465 (1989)], and scaling with the CH_4 trend. The H_2O difference is a result of CH_4 oxidation in the stratosphere.
17. The HNO_3 trend is estimated by assuming that the NO_y trend is the same as the N_2O trend (0.2%) and using the scaling of NO_y (*10*).
18. Projected injections of NO_y and H_2O are taken from scenario F in M. Prather *et al.* [*NASA Ref. Publ. 1272* (1992)]. In this report, NO_y is estimated to increase 4 ppbv and H_2O will increase by about 1 ppmv, for an emission index of 15 and a Mach number 3.2.
19. T. Peter *et al.* [*Geophys. Res. Lett.* **18**, 1465 (1991)] calculated a doubling of the PSC probability for future fleets of stratospheric aircraft (a 1.7 K increase in the 50-hPa NAT saturation temperature using a two-dimensional chemistry model).
20. We thank all the participants in the AASE II mission.

19 February 1993; accepted 13 July 1993

Chemical Loss of Ozone in the Arctic Polar Vortex in the Winter of 1991–1992

R. J. Salawitch, S. C. Wofsy, E. W. Gottlieb, L. R. Lait,
P. A. Newman, M. R. Schoeberl, M. Loewenstein, J. R. Podolske,
S. E. Strahan, M. H. Proffitt, C. R. Webster, R. D. May,
D. W. Fahey, D. Baumgardner, J. E. Dye, J. C. Wilson,
K. K. Kelly, J. W. Elkins, K. R. Chan, J. G. Anderson

In situ measurements of chlorine monoxide, bromine monoxide, and ozone are extrapolated globally, with the use of meteorological tracers, to infer the loss rates for ozone in the Arctic lower stratosphere during the Airborne Arctic Stratospheric Expedition II (AASE II) in the winter of 1991–1992. The analysis indicates removal of 15 to 20 percent of ambient ozone because of elevated concentrations of chlorine monoxide and bromine monoxide. Observations during AASE II define rates of removal of chlorine monoxide attributable to reaction with nitrogen dioxide (produced by photolysis of nitric acid) and to production of hydrochloric acid. Ozone loss ceased in March as concentrations of chlorine monoxide declined. Ozone losses could approach 50 percent if regeneration of nitrogen dioxide were inhibited by irreversible removal of nitrogen oxides (denitrification), as presently observed in the Antarctic, or without denitrification if inorganic chlorine concentrations were to double.

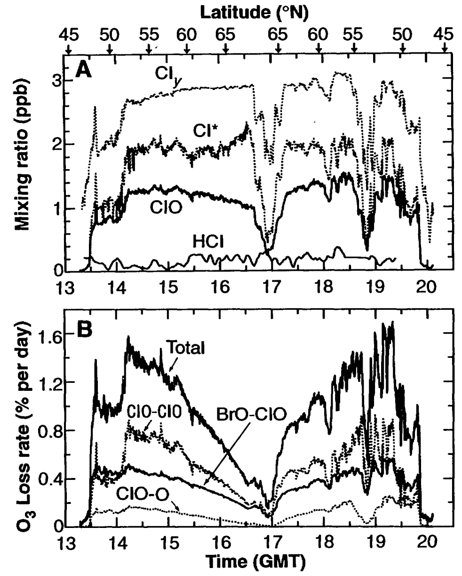

Fig. 1. Observations and reconstructions for 20 January 1992. (**A**) Observed mixing ratios of ClO and HCl, inferred mixing ratios for Cl* and Cl_y, and (**B**) the 24-hour mean loss rates for ozone, computed using Eq. 4 and Cl* shown in (A). The total recombination rate and contributions from the ClO-ClO, BrO-ClO, and ClO-O catalytic cycles (reactions 1, 2, and 3) are shown. All measurements taken along the ER-2 flight track, plotted against universal time (GMT). Corresponding latitudes are indicated at the top of the figure.

Loss rates for O_3 were estimated for the lower stratosphere during AASE II in 1991–1992. We computed distributions of reactive chlorine ($Cl^* \equiv [ClO] + 2 \times [(ClO)_2]$) and bromine ($Br^* \equiv [BrO] + [BrCl]$) (where brackets denote concentration) along the flight track of the ER-2 airplane by assimilating in situ observations of ClO and BrO with a simple model. Relations between potential vorticity (PV) and potential temperature (Θ), meteorological tracers (*1*, *2*), and Cl* and Br* were developed to compute O_3 loss rates for the north polar region, accounting for the influence of insolation, temperature, and pressure as air circulates around the polar vortex (*3*, *4*). Seasonal changes observed for ClO (*5*), NO (*6*), HCl (*7*), and O_3 (*8*) were investigated with the use of a photochemical model constrained by meteorological observations (9) and measured surface areas for sulfate aerosol (*10*); factors regulating chemical removal of O_3 in the Arctic were examined with this model.

Reactions on the surfaces of polar stratospheric clouds (PSCs) (*11*), which are composed of condensed phases of H_2O and HNO_3 (*12*), catalyze the rapid conversion of HCl and $ClNO_3$ to labile species of inorganic chlorine in the polar vortex during winter (*13*, *14*). Three catalytic cycles involving halogens account for ~95% of photochemical loss of O_3 in the vortex.

1) The self-reaction of ClO forming its dimer, $(ClO)_2$, followed by photolysis

$$\mathrm{ClO + ClO + M \rightarrow (ClO)_2 + M} \quad (1)$$
$$\mathrm{(ClO)_2} + h\nu \rightarrow \mathrm{ClOO + Cl}$$
$$\mathrm{ClOO \rightarrow Cl + O_2}$$
$$\mathrm{2(Cl + O_3 \rightarrow ClO + O_2)}$$
$$\mathrm{Net{:}\ 2O_3 \rightarrow 3O_2}$$

catalyzes the recombination of two O_3 molecules with the use of one photon (with energy $h\nu$) (*15*). Thermal decomposition of $(ClO)_2$ short-circuits this cycle, regenerating ClO without producing Cl atoms or recombining O_3.

2) The reaction of BrO and ClO and the photolysis of BrCl

$$\mathrm{BrO + ClO \rightarrow Cl + Br + O_2} \quad \mathrm{(2a)}$$
$$\rightarrow \mathrm{Br + OClO} \quad \mathrm{(2b)}$$
$$\rightarrow \mathrm{BrCl + O_2} \quad \mathrm{(2c)}$$
$$\mathrm{BrCl} + h\nu \rightarrow \mathrm{Br + Cl}$$
$$\mathrm{Br + O_3 \rightarrow BrO + O_2}$$
$$\mathrm{Cl + O_3 \rightarrow ClO + O_2}$$
$$\mathrm{Net\ (2a,\ 2c){:}\ 2O_3 \rightarrow 3O_2}$$

also catalyzes recombination of O_3 (*13*). Photolysis of OClO produces O atoms; therefore, reaction 2b does not destroy O_3 (*16*).

3) The reaction sequence

R. J. Salawitch, S. C. Wofsy, E. W. Gottlieb, Division of Applied Sciences and Department of Earth and Planetary Sciences, Harvard University, Cambridge, MA 02138.
L. R. Lait, P. A. Newman, M. R. Schoeberl, S. E. Strahan, National Aeronautics and Space Administration (NASA) Goddard Space Flight Center, Greenbelt, MD 20771.
M. Loewenstein, J. R. Podolske, K. R. Chan, NASA Ames Research Center, Moffett Field, CA 94035.
M. H. Proffitt, D. W. Fahey, K. K. Kelly, National Oceanic and Atmospheric Administration (NOAA) Aeronomy Laboratory, Boulder, CO 80303.
C. R. Webster and R. D. May, Jet Propulsion Laboratory, Pasadena, CA 91109.
D. Baumgardner and J. E. Dye, National Center for Atmospheric Research, Boulder, CO 80307.
J. C. Wilson, Department of Engineering, University of Denver, Denver, CO 80208.
J. W. Elkins, NOAA Climate Monitoring and Diagnostics Laboratory, Boulder, CO 80303.
J. G. Anderson, Departments of Earth and Planetary Sciences and Chemistry, Harvard University, Cambridge, MA 02138.